Available online at www.sciencedirect.com
SCIENCE DIRECT®
International Journal of Mass Spectrometry 225 (2003) 233–248
International Journal of Mass Spectrometry
www.elsevier.com/locate/ijms

Theoretical calculation of isotope effects, kinetic energy release and effective temperatures for alkylamines

László Drahos, Judit Sztáray, Károly Vékey*

Chemical Research Center, Hungarian Academy of Sciences, Pusztaszeri 59-67, H-1025 Budapest, Hungary

Received 6 August 2002; accepted 11 December 2002

Abstract

The kinetic isotope effect (KIE) and kinetic energy release (KER) of protonated alkylamine dimers were studied by theoretical modeling. In the calculations on reaction kinetics one empirical parameter was used to describe the looseness of the transition state. Calculations are compared to experiments described by Norrman and McMahon [Int. J. Mass. Spetrom. 182/183 (1999) 381]. In the case of experiments using a high-pressure ion source the Rice–Ramsperger–Kassel–Marcus (RRKM) model, taking into account energy distributions and the time scale of metastable ion fragmentation, accurately describes the experimentally observed KIE's of α-deuterated amines. The KER (available experimentally in one case only) is also correctly calculated, using no further parameters. In the case of low-pressure ion source, the internal energy distribution (IED) is not thermal, so it was empirically estimated based on the experimentally observed KIE. Using this estimate, it was possible to calculate the KER of α-deuterated amines accurately. Based on theoretical expectations it was found that the mean KER value is equal to $3/2kT_{\mathrm{eff}}$. This allows estimation of the KER in cases where it is determined by statistical factors. Energy distributions of various fragmenting ion populations are discussed in some detail. These may be helpful for a qualitative understanding of mass spectrometric processes and the theoretical basis of the kinetic method.

Keywords: Kinetic isotope effect; Kinetic energy release distribution

1. Introduction

Kinetic isotope effects (KIEs) of gas phase reactions have been studied extensively using mass spectrometry [1–12] yielding detailed information on the structure of gaseous ions and neutrals and also on reaction mechanism [3]. In many cases primary hydrogen KIEs were investigated, but secondary isotope effects are often also significant [3,7–9]. Recently, the isotope effect in dissociation reactions of proton-bound amine dimers have been characterized in detail. The proton-bound labeled–unlabelled amine dimer may loose either an unlabelled or a labeled amine neutral as shown in Eqs. (1a) and (1b) in the case of methylamine.

$$[CH_3NH_2 \ldots H^{\oplus} \ldots CD_3NH_2] \rightarrow CD_3NH_3^{\oplus} + CH_3NH_2, \quad k_H \tag{1a}$$

$$[CH_3NH_2 \ldots H^{\oplus} \ldots CD_3NH_2] \rightarrow CH_3NH_3^{\oplus} + CD_3NH_2, \quad k_D \tag{1b}$$

The ratio of the respective reaction rates (k_H/k_D) was found to be larger than unity, indicating a normal

* Corresponding author. Tel.: +36-1-4380481; fax: +36-1-3259105.
E-mail address: vekey@chemres.hu (K. Vékey).

1387-3806/02/$ – see front matter © 2002 Elsevier Science B.V. All rights reserved.
doi:10.1016/S1387-3806(02)01117-X

secondary isotope effect. This also means that the proton affinity of deuterated amines is higher than that of unlabelled amines. These reactions were studied very carefully by Norrman and McMahon [9], using a variety of mass spectrometric techniques. This is ideal ground for the application of Cooks and co-worker's kinetic method [13–15], because its assumptions are most likely to be satisfied due to the close similarity of the two monomers. The kinetic method has been a center of intensive debate in recent years [15–17]: whether or not it is only an empirical method or can it be theoretically derived [18–21]; what is the meaning of the effective temperature [17,19–22], and how accurate are thermodynamic data derived using this technique [23,24]. To highlight some of these points we have decided to calculate isotope effects theoretically in the case of proton-bound alkyl amines.

The direction and size of the KIE has been calculated in a number of cases [3,5,12,25]. In a very detailed paper, Schwarz and co-workers [12] discussed various processes contributing to the KIE. Probably the most important is the difference in zero point vibrational energy (ZPE). This can be determined usually quite accurately by quantum chemical calculations. Knowing the differences in energy levels, the KIE can be calculated in thermal systems. In a not-thermal case (like a mass spectrometer) it is less straightforward to determine parameters necessary to calculate KIE (e.g., initial internal energy distribution (IED), angular momentum of precursor ion).

The kinetic energy release (KER) is an important quantity characterizing reactions. This can be measured experimentally from the width and shape of metastable peaks, and yields valuable information on ion structures, transition states and reaction dynamics. The measurement and evaluation of KER has been subject of detailed studies and reviews [26–31]. There are several theoretical approaches to calculate the KER of reactions: the statistical energy partitioning prior to distribution [26], phase space theory (PST) [32,33], orbiting transition state phase space theory (OTS/PST) [34,35], finite heat bath theory [20,36,37] (FHBT) [20,36,37] and the maximum entropy method [38–40]. Note the particularly good agreement between experimental and calculated KER(D) curves obtained by the OTS/PST approach [41]. Recently, FHBT has been successfully used to study the theoretical basis of the kinetic method [20]. Each of these theories involves different approximations and assumptions. The discussion of various models for calculating the KER is outside the scope of the present paper; it can be found in excellent books and reviews [26–28].

In our studies on KIE and KER we have used the MassKinetics algorithm. It is a general framework for modeling mass spectrometric processes, discussed in detail recently [42]. It combines modeling reaction rates, energy exchange processes in the gas phase and the calculation of product ion abundances as the ions move through various parts of a mass spectrometer. In MassKinetics ions are characterized by their internal and kinetic energies, which define the 'state' of an ion. Essential features of the model are the use of internal (and, if necessary kinetic) energy distributions and the use of probabilities to describe transition between different states. Reaction rates are calculated based on the transition state theory (TST) in its Rice–Ramsperger–Kassel–Marcus (RRKM) formulation [26,43,44]. The kinetic and/or internal energies of ions in the gas phase may change due to (a) acceleration in electromagnetic fields, (b) radiative energy exchange (photon absorption and emission), (c) collisional energy exchange, and (d) energy partitioning in chemical reactions, which are all taken into account. Note that among these, collisional energy exchange may be described using different collision models. Energy exchanges processes and fragmentation take place in the same time frame, which is taken into account using so-called master-equations [45]. While the mathematical description of these physical processes is quite complex, it has the immense advantage that ion abundances can be calculated accurately using very few empirical or adjustable parameters [19,46,47].

In the present paper, results on small alkylamines (methylamine, ethylamine, dimethylamine, methylethylamine, diethylamine, methyl-propylamine, methyl-butyl-amine and deuterated analogues) are studied. The calculated KIE and KER values are compared with experiments performed by Norrman and

McMahon [9]. Most parameters used in modeling have been taken from this paper, the rest was calculated by quantum chemical calculations. The only empirical parameter in the simulation of high-pressure experiments was the pre-exponential factor, used to describe the transition state (TS). The same pre-exponential factor was used for all compounds in the present study. While thermal energy distribution is likely to be a good approximation for high-pressure ion source, in low-pressure sources it would be significantly different. To model experiments in the latter case the IED was adjusted empirically to match the experimentally observed KIE. This energy distribution was used subsequently to calculate the KER.

2. Details of calculations

Calculations have been performed using the MassKinetics Scientific (Ver. 1.2) software, which is a more powerful version of MassKinetics Demo (Ver. 1.2), available at www.chemres.hu/ms/masskinetics. Calculations presented in this communication can also be downloaded from its web site, allowing further calculations or tests on these amine systems to be performed by the interested reader. As described, the internal energy is defined as the sum of vibrational and internal rotational energy of the molecule above the ZPE. The overall rotational energy of the molecule is treated separately, as it cannot freely interconvert with the vibrational energy due to angular momentum conservation. In the present calculations, the following numerical approximations are used: in RRKM calculations the harmonic oscillator model is applied, internal rotations are approximated by low frequency vibrations (as calculated by quantum chemistry). Energy partitioning is based on statistical distributions (far superior to equipartitioning). In the case of energy partitioning, rotations are explicitly considered using the classical rotor approximation. As experiments relate to metastable ions (i.e., spontaneous fragmentation), collisional excitation is not considered. It was checked that 30 times faster cooling than that specified by Dunbar's standard hydrocarbon model [48], the influence of radiative cooling on fragmentation rates is less than 0.1% and even less for the isotope effect and for kinetic energy release. For this reason radiative cooling was neglected. Vibrational frequencies were specified with an accuracy of 1 cm^{-1}. Precision of calculations was defined to provide better than 0.01% numerical precision of all calculated parameters. In such conditions calculations for one compound require 1–10 s on a typical PC.

In the calculations the experiment was defined in the following way. The ions are formed in the source at thermal equilibrium (450 K, defining the internal and kinetic energy distributions). It was checked that using 50 K lower and higher source temperature in model calculations, the influence of source temperature on KIE and KER is less than 1%. They are accelerated to a few keV kinetic energy (depending on the experimental conditions) and traverse the first part of the instrument, where mass selection takes place. Only the precursor ion (the protonated alkylamine dimer) enters the field free-region (FFR), where metastable (i.e., unimolecular) fragmentation takes place. The product distribution at the end of the FFR represents the mass spectrum discussed.

The modeling requires, beside the instrumental parameters discussed above, the reaction enthalpy (ΔH°) and vibrational frequencies. The reaction enthalpy was taken from the literature (Table 2 in [9]). For methyl-propylamine, and methyl-butylamine ΔH° values are not available. For these compounds the binding energy was estimated by extrapolation (23.7 and 23.6 kcal/mol) based on data given in the aforementioned table. The accuracy of these values is estimated to be ±1 kcal/mol (compared to ±0.1 kcal/mol accuracy of the ΔH° values quoted in [9]). Model calculations indicate that this results in ±0.003–0.005 uncertainty in the theoretically calculated isotope effect, significantly less than the experimental uncertainty.

Vibrational frequencies for proton bound complexes, product ions and neutrals were determined using high quality quantum chemical techniques. For most compounds these were calculated at the MP2/6-31G(d,p) level by Norrman and McMahon [9], and

were kindly provided. For the proton-bound dimers of methyl-propylamine, methyl-butylamine and for the methyl-ethylamine and diethylamine analogues were determined at the B3-LYP/6-31G(d,p) level [49–51], after full geometry optimization. For determining ZPEs, the calculated frequencies were scaled using the values suggested [52,53] (0.9608 for MP2/6-31G(d,p) and 0.9806 for B3-LYP/6-31G(d,p)). RRKM calculations and statistical energy partitioning use the same vibrational frequencies, but in these cases low frequency modes have a larger influence. For this reason in RRKM and in energy partitioning the scaling factors optimized for low frequency vibrations [53] have been used (1.0229 for MP2/6-31G(d,p) and 1.0013 for B3-LYP/6-31G(d,p)). To reduce numerical errors, input parameters, conversion units and scaling factors with at least five significant digits were used in all calculations. The results were rounded to a chemically reasonable accuracy only when reporting the data in the paper.

Proton-bound dimers and ion–dipole complexes are known to dissociate through loose, product-like transition states (TS) [9,18,19,26]. The looseness of the TS is characterized by a single parameter, the Arrhenius-type pre-exponential factor (A_{preexp}). The TS is defined by molecular frequencies of the products and five 'cluster modes', the sixth being the reaction coordinate. Among them one is a rotation (which is assumed to be unchanged), the frequency of the other four vibrations is reduced in the TS [17,54]. Using the value $\lg A_{\text{preexp}} = 15$ suggested for proton-bound alcohols [18], calculations gave good results for proton-bound alkylamines as well. Optimizing A_{preexp} for the transition state of reaction (1a) and for the analogous dissociations leading to neutral-unlabelled amine ("a" processes), the best agreement between calculated and measured KIE values was obtained using $\lg A_{\text{preexp}}(\text{a}) = 15.4$. The Arrhenius factor so determined is typical for loose TSs [18,19,26]. Note that the same $A_{\text{preexp}}(\text{a})$ was used for all compounds studied in the present paper. To check the influence of this empirical estimate on the results, calculations were repeated using 10 times larger and 10 times lower pre-exponential factors as well. $A_{\text{preexp}}(\text{b})$, corresponding to the reaction leading to neutral labeled amine (process "b") is determined from $A_{\text{preexp}}(\text{a})$ and the respective product frequencies, without using any further parameters. As product frequencies corresponding to the two reaction channels ($CH_3NH_3^+$ and CD_3NH_2 on the one hand, and $CD_3NH_3^+$ and CH_3NH_2 on the other hand) are different, the frequency factors will also differ by a small amount. This is an entropy effect, in the case of methylamine this favors reaction (1a) over (1b) by 5.5%. (This would be the isotope effect at infinitely high internal energy.) This is equivalent to a 0.08 cal/mol K entropy difference in a thermal system (at 600 K), which agrees reasonably with the 0.1–0.2 cal/mol K $\Delta\Delta S$ values experimentally determined. Note that the 5.5% quoted here has been calculated for methylamine-d3-methilamin dimer, for other compounds it is a different value.

In [9] two experimental setups are used, one on a VG 70-70, the other on a JEOL JMS-HX110/HX110A instrument. From the flight times of ions given in Norrman's paper, the geometry of VG instrument can be deduced (length of the flight path up to the FFR and length of the FFR in which fragmentation is observed, 1.1 and 0.3 m, respectively). These parameters define the time-scale of the experiments for all ions concerned. In the case of JEOL instrument, the ions are accelerated to 10 kV, the instrument geometry (determined from the flight time as well) is 2.5 m up to the FFR and the length of the FFR is 1.5 m. The time-scale is slightly longer on the JEOL compared to the VG instrument.

3. Results and discussion

3.1. Modeling kinetic isotope effects

The method used to model mass spectra including isotope effects can be well illustrated in the case of the fragmentation of the proton-bound methylamine dimer (Eq. (1a) and (1b)). To calculate characteristics of this reaction, molecular parameters and thermodynamic data of the reaction are needed as described above. The reaction enthalpy (ΔH°) for reaction (1a)

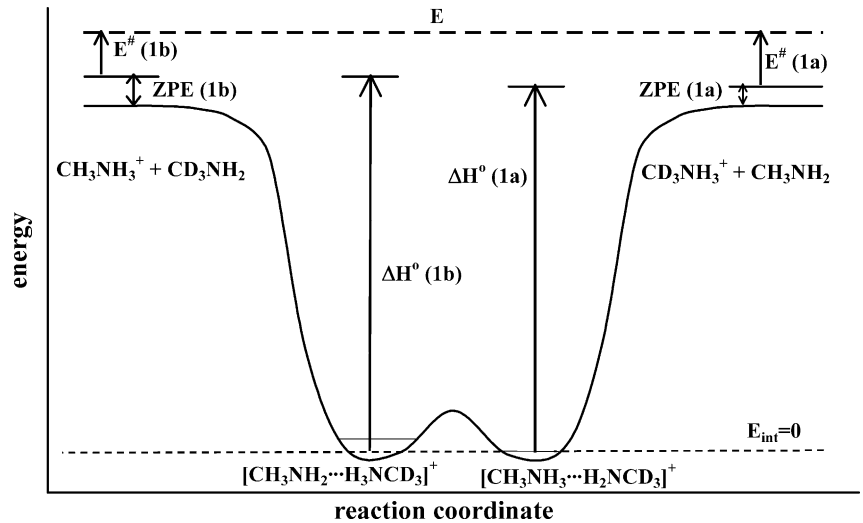

Fig. 1. Schematic potential energy diagram of the fragmentation of protonated methylamine dimer.

is 26.9 kcal/mol, taken from Table 2 of [9]. The reaction enthalpy of (1b) can be determined from that of (1a) and from the difference of ZPEs (calculated in turn from the vibrational frequencies), as qualitatively shown in Fig. 1. Note that in the calculation only one complex was calculated and rapid interconversion between two structures was assumed. The ΔH° for reaction (1b) is 0.128 kcal/mol (5.56 meV) larger than that for reaction (1a). Fig. 1 also illustrates that the excess energy ($E^{\#}$) is the difference between the internal energy (E) and the reaction enthalpy.

Due to angular momentum conservation part of the overall rotational energy of the molecule may be converted into internal energy. While this can properly be considered, the rotational energy (the distribution of rotational quantum states to be more precise) is almost never known in the case of mass spectrometric experiments. Thermal distribution of rotational quantum states is usually assumed, which may be a good approximation in a thermal system (e.g., in the ion source), but electrostatic acceleration and collisions (e.g., while the ions are getting out of the source) can change it significantly. To keep the model simple, it was assumed that the overall rotational energy will not change between the precursor and the transition state.

The next step in the modeling is definition of the mass spectrometric experiment. In [9] two experimental setups are used, one on a VG 70-70, the other on a JEOL JMS-HX110/HX110A instrument. The two experimental setups gave quite different results, suggesting that one may be suspect. First, experiments on the VG system will be modeled. In this case, a high-pressure ion source was used. It is reasonable to assume that ions will have a thermal energy distribution in such a case. No temperature dependence of the isotope effects was observed in the 300–500 K range of source temperatures [9]. As most experiments were performed between 400 and 500 K, 450 K source temperature was used in the modeling. The ions were accelerated to 2900 eV and the protonated dimer was selected. The metastable fragmentation of this ion was studied by mass analyzed ion kinetic energy spectroscopy (MIKES).

Based on the parameters specified above mass spectrometric features of the protonated methylamine dimer can be calculated. Calculations were repeated using significantly 10 times larger and 10 times lower pre-exponential factors as well, which represents error limits of the calculation. This results in a different isotope effect (and KER) and this range is indicated by the error limits of the calculated KIE values. In the

case of methylamine, the isotope effect is calculated to be 1.43 (error limit: 1.33–1.61), which compares favorably with the experimentally measured value of 1.39. Based on the calculated ion ratio (1.43), and knowing the ΔH difference between reaction channels (1a) and (1b) the 'effective temperature' can be calculated based on the fundamental equation of the kinetic method [13]:

$$\ln\left(\frac{k_H}{k_D}\right) \approx \ln\left(\frac{I_H}{I_D}\right) = \frac{\Delta\Delta H_0}{RT_{eff}} = \ln \mathrm{KIE} \qquad (2)$$

This results in 179 K effective temperature for the protonated methylamine dimer (range of 134–225 K using the error limits as described above). Like the isotope effect, this is also reasonably close to the 194 K value determined experimentally.

Fragmentation of other α-D substituted alkylamines has also been studied, the KIEs are shown in Table 1. The results indicate good agreement between the calculated and measured KIE values determined using the high-pressure ion source. Correlation between experimentally observed and theoretically calculated KIEs are also shown in Fig. 2. The mean standard deviation of experimentally observed and theoretically calculated KIEs (0.020) is only two times larger than the experimental uncertainty of the measurements (0.010).

The good agreement between the experimentally observed and calculated KIEs rests on three conditions: (1) accurate experiments under well-defined, thermal conditions; (2) accurate calculation of fragment abundances; and (3) accurate quantum-chemical calculation of frequency changes due to deuteration. The agreement is good for α-D substitution, but it is not to for β-D substituted alkylamines (Table 1 and full circles in Fig. 2). As noted by Norrman and McMahon [9], α- and β-D substituted alkylamines show experimentally fairly similar KIEs, but the corresponding energy difference (calculated by quantum chemistry) is ca. 4 times lower in the case of β substitution. Our calculations support the previous tentative suggestion [9], the experimentally observed KIEs for β-D substituted amines are not possible to explain based on ab initio calculated ΔZPE(H/D) values. The reason of apparent failure of ab initio calculation at the MP2/6-31G(d,p) level is not clear, but note that the energy difference is very small. As experiments and ab initio calculations are in disagreement for β-D substituted alkylamines, those compounds are not considered for further calculations here.

In the second experimental setup (JEOL instrument) low-pressure ionization has been used. The experimental result shows a much larger isotope effect

Table 1
Experimental data and results of calculations for dissociation reactions of proton-bound dimers B–H^+–B-dn

B-dn	VG k_H/k_D		JEOL k_H/k_D		JEOL (meV) ⟨KER⟩	
	Experimental	Calculated[a]	Experimental	Calculated[a]	Experimental[b]	Calculated[c]
CD_3NH_2	1.39	1.43 (1.33–1.61)	4.10	1.45 (1.34–1.65)	5.3	3.6 (3.6–4.4)
$CD_3NH–CH_3$	1.28	1.24 (1.20–1.29)	1.63	1.25 (1.21–1.30)	16.3	17.7 (16.2–20.1)
$CD_3NH–C_2H_5$	1.22	1.20 (1.18–1.25)	1.36	1.21 (1.18–1.25)	24.5	29.2 (27.2–31.7)
$CD_3NH–C_3H_7$	1.19	1.18 (1.16–1.20)	1.30	1.18 (1.17–1.20)	28.4	31.9 (30.5–32.5)
CD_3NH-*n*-C_4H_9	1.16	1.17 (1.16–1.19)	1.26	1.21 (1.19–1.24)	33.2	36.6 (35.2–36.9)
$CH_3CD_2NH_2$	1.16	1.19 (1.16–1.23)	1.30	1.19 (1.16–1.24)	19.4	28.3 (25.7–31.0)
$CH_3CD_2NH–CH_3$	1.14	1.17 (1.15–1.21)	1.24	1.17 (1.15–1.21)	24.5	35.5 (32.7–38.5)
$CH_3CD_2NH–C_2H_5$	1.12	1.15 (1.13–1.16)	1.25	1.15 (1.13–1.16)	28.6	31.4 (29.5–32.0)
$CD_3CH_2NH_2$	1.17	1.07 (1.06–1.09)	1.18	1.07 (1.06–1.09)	20.2	14.9 (13.4–18.3)
$CD_3CH_2NH–CH_3$	1.15	1.05 (1.04–1.06)	1.13	1.05 (1.04–1.07)	24.6	15.3 (14.2–18.3)
$CD_3CH_2NH–C_2H_5$	1.13	1.04 (1.04–1.04)	1.13	1.04 (1.04–1.04)	29.8	15.0 (15.4–16.0)

[a] Calculated assuming thermal energy distribution when ions leave the ion source.
[b] Recalculated form data in [9].
[c] Calculated using a non-thermal energy distribution for the precursor ion. In the calculation the internal energy distribution was changed from thermal to such a distribution, which yields the KIE experimentally observed on the JEOL instrument (described in detail in the text).

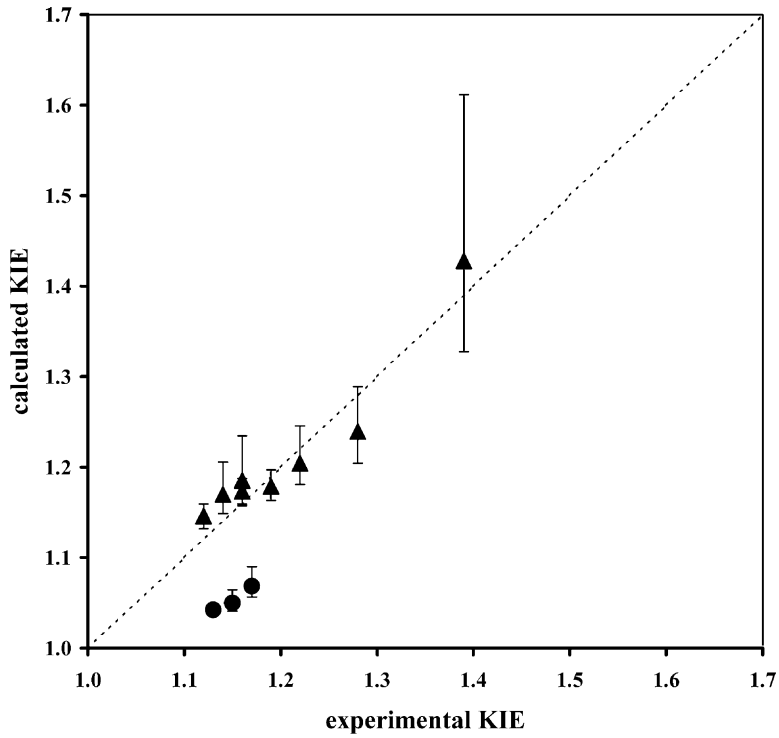

Fig. 2. Correlation between the experimentally measured and theoretically calculated KIE on the VG instrument. The error bars indicate the calculated KIE using 10 times lower and higher pre-exponential factor. Triangles relate to α-D substitution (correlation coefficient is 0.953), circles to β-D substitution. The dashed line represents exact agreement between experiments and calculations.

($k_H/k_D = 4.10$ for methylamine) in low-pressure ionization, than in the high pressure experiments discussed above. The experimentally observed isotope effect (KIE = 4.10) corresponds to a very low effective temperature (44 K as defined by Eq. (2)), and clearly illustrates a large difference in the internal energies of reacting ions. When thermal energy distribution is assumed for the case of low-pressure ionization, the calculation indicate that the isotope effect would be 1.45 ($T_{eff} = 172$ K), similar to that observed in the other instrumental setup, but far lower than that determined experimentally. Analogous results were obtained for other α-D substituted alkylamines as well (Table 1). The simplest explanation is that the IED in the low-pressure ion source is not thermal. This possibility was noted by Norrman and McMahon as well [9]. This conclusion is corroborated by other evidence as well. If IED in the low-pressure ion source were thermal, the higher KIE would indicate a lower temperature. This, in turn, would result a lower degree of fragmentation. In contrast, the experiments show [9] that fragment ion yield is much higher in the JEOL instrument using the low-pressure ion source. An alternative explanation is that a difference in the time-scale of the two instruments causes the variation in the isotope effect. Model calculations indicate that the difference in time-scales is small, and have a very small influence on the results. Note that the taking the time-scale into account is straightforward and accurate.

Internal energy distribution in the low-pressure ion source should satisfy two criteria: fragment ion abundance should be higher, while effective temperature should be much lower than that in the case of the high-pressure ion source. High fragment ion abundance means that a larger fraction of ions have internal energy above the fragmentation threshold. The low

effective temperature means that the energy distribution must be very narrow above the fragmentation threshold. Note that qualitatively such a distribution can be expected based on the ion formation mechanism, assuming that the number of collisions is not sufficient to obtain true equilibrium in the low-pressure ion source. The first step is formation of protonated methylamine, which reacts with neutral methylamine. The newly formed methylamine-protonated methylamine complex will stabilize only if the internal energy is just above the binding energy and energy dissipation by collisions occurs. This will result in an initially narrow energy distribution for the dimer, with a mean value slightly above the binding energy of the complex. Such an internal energy distribution would result in a high fragment ion yield and a low effective temperature. When complex undergoes collisional cooling, the IED will change and will become more similar to a thermal distribution. Until true equilibrium is not reached, the energy distribution will be characterized by a higher than thermal fragmentation rate and a lower than thermal effective temperature, as observed experimentally. We are in the process to extend MassKinetics to be able to model collisional cooling processes in the ion source and to have the ability to follow internal energy changes in a quantitative manner. Empirically, this could be modeled by an internal energy distribution decaying exponentially above the binding energy of the complex. This requires one parameter, which may be determined from the experimentally observed KIE.

At this point it may be instructive to discuss the calculated internal energy distributions. Thermal IED of protonated methylamine dimer is shown in Fig. 3 at 400 and 450 K. The fragmentation threshold (1.1670 eV) is only slightly above the critical energy (1.1665 eV) of the lower energy channel. (Note that the critical energy is taken from [9], the four decimal units are a consequence of energy conversion from kcal to eV units.) The fragmentation threshold is always higher than the critical energy, the difference is usually defined as the kinetic shift. The probability of precursor ions to be above 1.16 eV internal energy is very low both at 400 and 450 K, so this part of the distribution is blown up by 1000 times in Fig. 3. The tails of the distributions are similar, suggesting that the

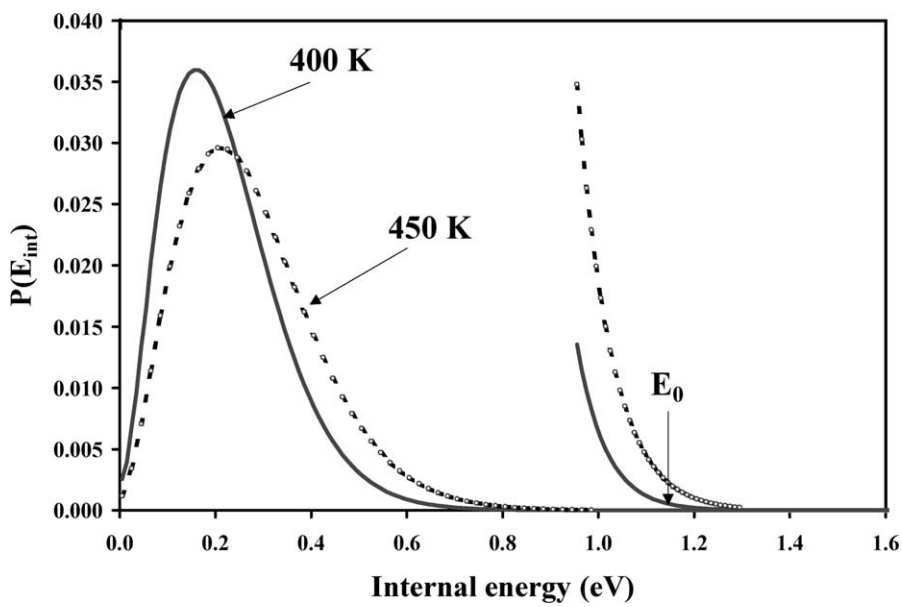

Fig. 3. Thermal internal energy distributions of protonated methylamine dimer at 400 K (solid line) and 450 K (dotted line) temperature. The tails of the distributions are shown in a 1000 times magnified scale. E_0 indicates the critical energy of the lower energy channel.

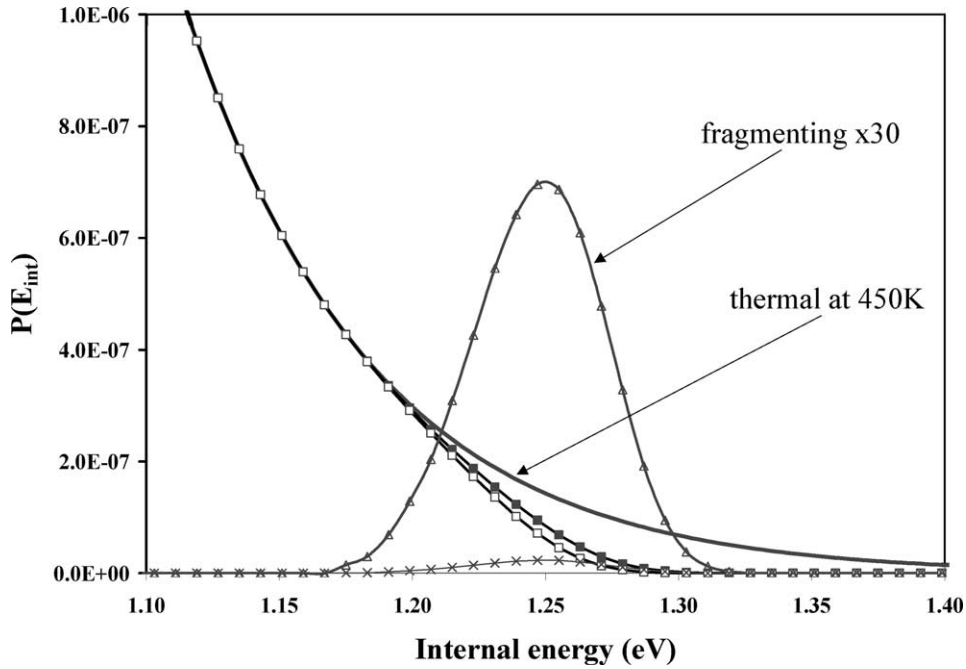

Fig. 4. The high energy tail of internal energy distribution of protonated methylamine dimer using high-pressure ion source at 450 K source temperature. The thermal distribution is shown by the continuous line. Full squares show the distribution related to ions reaching the FFR, open squares those leaving the FFR intact. The difference between these two distributions (shown by crosses) represents ions fragmenting in the FFR, yielding MIKES products (also shown magnified by 30 times, indicated by triangles). Using Eq. (2) and the calculated fragment ion ratio $T_{eff} = 179$ K is obtained.

effective temperature and the size of the kinetic isotope effect will not depend on the source temperature significantly (which was also observed experimentally [9]). On the other hand, the tail at lower temperature is smaller, suggesting that the fragment ion yield will be much reduced at low source temperature. (Personal communication from McMahon indicates that indeed this was observed experimentally.)

Fig. 4. shows the IED of various fractions of protonated methylamine dimers in the 1.1–1.4 eV range using VG instrument (high-pressure ion source). Thermal IED at 450 K is shown by the solid line. A significant portion of high-energy ions will decompose before they reach the FFR. For this reason the probability of high-energy ions reaching the FFR (full squares in Fig. 4) will be significantly reduced compared to that of thermal distribution. The difference between the distribution of ions entering (full squares) and leaving the FFR (open squares) corresponds to the internal energy distribution of those protonated methylamine dimers, which do fragment in the MIKES experiment (indicated by crosses and also shown enlarged 30 times indicated by triangles). The figure illustrates that metastable ions represent only a small fraction of all parent ions (area under respective curve) and will have a fairly wide energy distribution. Ions fragmenting through the two competitive reaction channels (1a and 1b) have different IEDs, but the difference is so small, that it cannot be shown in Fig. 4. The effective temperature, determined using Eq. (2), characterizes this fragmenting ion population. The experimental data (KIE = 1.39) yields 194 K, the calculated value (KIE = 1.43) results in 179 K effective temperature.

In the case of modeling low-pressure ion source results (Fig. 5), the initial IED (solid line) was determined empirically to result in a KIE equal to that

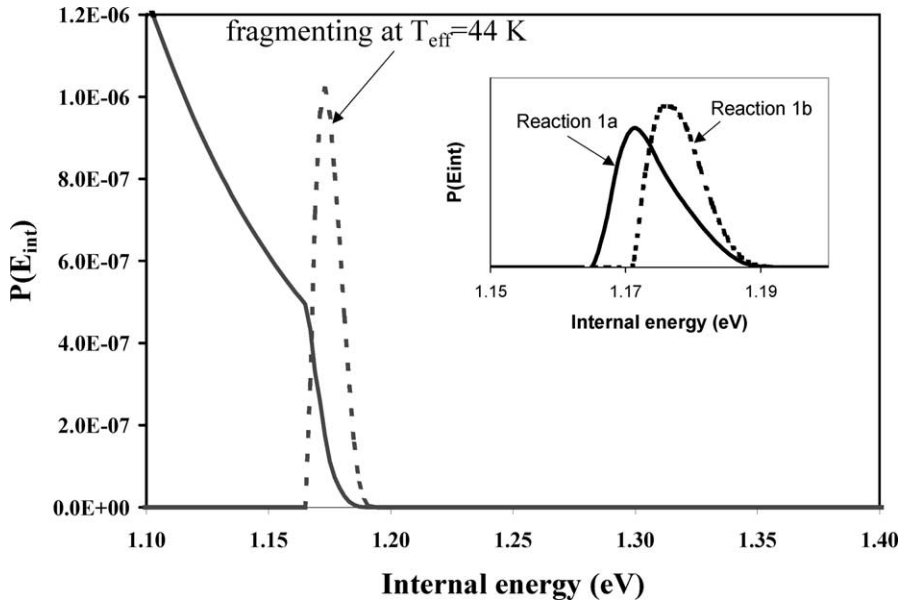

Fig. 5. High-energy tail of the internal energy distribution of protonated methylamine dimers reaching the FFR (solid line), and that of ions fragmenting inside the FFR (dashed line) on the JEOL instrument. The distribution is empirically obtained to result in 44 K effective temperature. Note that only the part above the fragmentation threshold ($E_0 = 1.167$ eV) is significant in this respect. The insert shows the internal energy distributions of ions fragmenting through reactions (1a) and (1b) (solid and dashed lines in the insert, respectively).

obtained experimentally (4.10). As discussed in [9] this corresponds to 44 K effective temperature. The shape of the IED below the fragmentation threshold (1.167 eV) has no relevance to fragmentation. Note that the distribution drops down very fast above the fragmentation threshold and there are practically no ions over 1.19 eV internal energy. The distribution of ions fragmenting inside the FFR is very narrow, shown by the dashed line in Fig. 5. We have tried several other trial distributions, all those capable of yielding $T_{\text{eff}} =$ 44 K were fairly similar to that shown in Fig. 5. The IED of fragmenting ions was always a narrow peak between E_0 (1.167 eV) and 1.19 eV, irrespectively on the precise shape of the initial internal energy distribution.

The insert in Fig. 5 shows the IED of fragmenting ions in a narrow energy range; here the ion population corresponding to the two competing channel (1a and 1b) are shown separately. The distribution related to (1b) is shifted by ~0.005 eV to higher energy—this value is very close to the difference between ΔH° of the two reaction channels (see insert in Fig. 5). This difference in the two distributions will influence the kinetic energy release observed for the two reaction channels, as will be discussed below. Note that the difference in the two ion populations quite large at this low effective temperature (44 K). As noted above, at higher effective temperatures (like at 179 K shown in Fig. 4) the difference between energy distributions corresponding to the two reaction channels (1a) and (1b) is very small. As a consequence, KER(H) and KER(D) values will also be very close in most cases. When not mentioned separately, the average of these two will be used throughout the paper.

It is also instructive to compare IED of ions fragmenting in a mass spectrometric experiment with those occurring under thermal (i.e., equilibrium) conditions. Ion produced in a high-pressure source at 450 K source temperature result in 179 K effective temperature according to model calculations. This is close to the experimentally determined effective temperature ($T_{\text{eff}} = 194$ K). Note that in this case the source and effective temperatures are significantly different. The

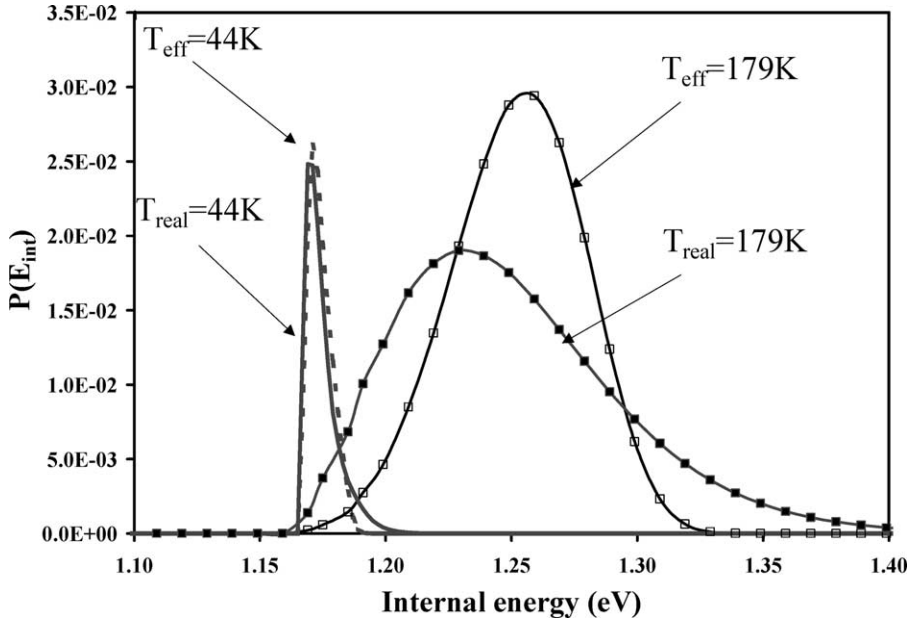

Fig. 6. Comparison of the calculated internal energy distribution of fragmenting protonated methylamine dimers characterized by 179 K (as observed in the high-pressure source) and 44 K (as observed in the low-pressure ion source) effective temperatures (full squares and dashed line, respectively) with that of ions reacting in a thermal system (at the high-pressure limit) characterized by 179 and 44 K "real" temperature (open squares and continuous line, respectively).

effective temperature in metastable fragmentation should be always lower, than initial temperature of ion source [17,24]; this is a consequence of ion fragmentation occurring inside mass spectrometer. IED of fragmenting ions at 179 K effective temperature (full squares in Fig. 6) can be compared to that of decomposing ions in a "real" thermal system (thermodynamic system at high-pressure limit, open squares in Fig. 6). The distributions start at the critical energy (as no ion below the critical energy can decompose) and continues to (in principle infinitely) high internal energy. The ions decomposing in a thermal system (179 K "real" temperature) and in a mass spectrometer (yielding 179 K T_{eff}) have fairly similar, but not identical distributions. The similarities of such distributions were observed for other alkylamines and other temperatures as well. Fig. 6 illustrates the methylamine system at 44 K as well: the full line shows the thermal distribution, the dashed curve the metastable distribution. As thermal and mass spectrometric distributions are not identical is a nice demonstration that the kinetic method is not a thermal experiment. Nevertheless, the roughly similar shape of the curves provides in our opinion qualitative support for the kinetic method (at least in case of metastable ions).

3.2. Modeling the kinetic energy release (KER)

As mentioned in Section 1, there are several theoretical models to calculate KER and KER distributions. In the present work we used the model mentioned as 'microcanonical prior distribution of product energies', as discussed by Baer and Hase [26]. This model assumes statistical energy partitioning among the products and their relative translational and rotational degrees of freedom, which implies that KER is due to a three-dimensional translational motion. One consequence of this assumption is that this model predicts a particular KER(D), which would produce an almost exact Gaussian-shaped metastable peak. In the

study of Norrman and McMahon [9], which forms the experimental basis of the present work, peak shapes are approximately Gaussian, but their detailed analysis was not performed. Preliminary work in our laboratory on fragmentation of protonated clusters [55] clearly show that in many cases the metastable peaks indeed have a Gaussian shape, which converts to a KER distribution described by three-dimensional translational energy distribution. These results tentatively support the choice of the model used in the present study. As discussed above conservation of angular momentum is not considered in our calculations. With the exception of very small molecules, this is often a good assumption for dissociation of ion–molecule complexes [28]. Our preliminary data on protonated clusters indicate that their KER distributions are practically identical with statistical (three-dimensional) kinetic energy distribution (Boltzman distribution).

Determination of the kinetic energy release is a particular case of energy partitioning. Statistical energy partitioning is used (which can be derived from assumptions deriving statistical reaction kinetic models, like RRKM), which is a good approximation when there is no reverse activation energy. Fig. 7 illustrates the result in the case of the protonated diethylamine dimer, under the experimental conditions observed on the VG instrument (high-pressure source). The internal energy distribution of parent ions fragmenting in the FFR is shown by full squares; that of the product ion by the dashed line; the relative translational motion (i.e., the KER distribution) by the solid line (the relative rotational energy of the two products and the internal energy of the product neutral is not shown). The shape of the KER is qualitatively fairly similar to a Maxwell–Boltzmann distribution (the kinetic energy distribution of gas molecules in a thermal system). Such distributions will result in approximately Gaussian-shaped metastable peaks. Note also that the internal energy distribution of the product ion is not smooth at low energy—this is a consequence of the quantized nature of oscillators. (The KER distribution is smooth, as translational energy levels are very

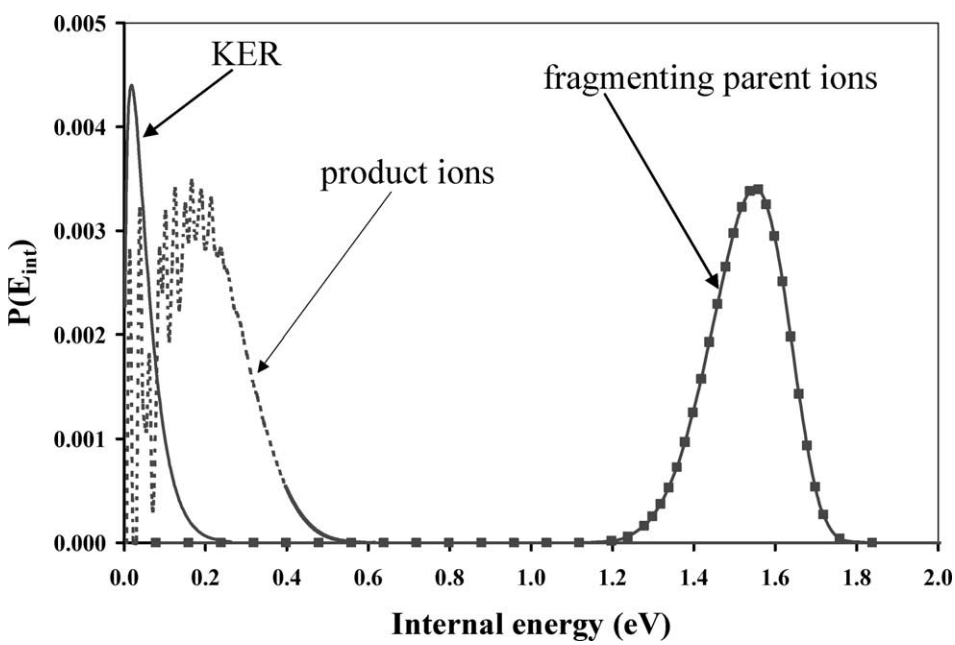

Fig. 7. Calculated energy distributions resulting from statistical energy partitioning in the case of the protonated diethylamine dimer, under experimental conditions observed on the VG instrument. Internal energy distributions of fragmenting parent ions (full squares), product ions (dashed line) and the kinetic energy release distribution of fragment ions (solid line) are shown.

close.) The mean excess energy ($E^{\#} = E - E^{\circ}$) in this case is 0.49 eV; in the case of low pressure ionization it is much smaller, 0.20 eV. Assuming equipartitioning, the excess energy can be estimated independently from T_{eff} and from KER, as pointed out by Norrman and McMahon [9]. Note that equipartitioning may be regarded as an approximation of statistical energy partitioning. The calculations result in $E^{\#} = 1.6$ and 1.2 eV, respectively, in the case of low pressure experiments [9]. Compared to the case of statistical energy partitioning this overestimates the amount of excess energy by nearly 10 times. This suggests that equipartitioning should be used with sufficient caution in cases, when the degree of excitation is relatively low.

It is well established that the mean KER value and that determined at half-height of the metastable peak ($\langle \text{KER} \rangle$ and $\text{KER}_{0.5}$) are different. For Gaussian-shaped metastable peaks the ratio is exactly known as [56]:

$$\langle \text{KER} \rangle = 2.16\, \text{KER}_{0.5} \tag{3}$$

KER data in Norrman and McMahon's paper has mostly been determined on the JEOL instrument (probably due to its better resolution). Only one example is given using the high-pressure ion source on the VG instrument (Fig. 8 in [9]) corresponding to the fragmentation of protonated diethylamine. From the peak shape given there the $\text{KER}_{0.5}$ value is 31 meV; and the peak is (approximately) of Gaussian shape. The mean $\langle \text{KER} \rangle$ value is consequently 67 meV. Note that this value is likely to be an upper limit for $\langle \text{KER} \rangle$, as the influence of peak broadening due to instrumental effects (like the width of the ion beam) was not taken into account. Using the same ± 1 order of magnitude uncertainty in the pre-exponential factor as discussed before, the calculated $\langle \text{KER} \rangle$ value falls into the 47–54 meV range. Note that, this calculation uses no empirical parameter beside the pre-exponential factor, so we believe that it is a fair agreement.

KER data for other alkylamines are available [9] obtained on the low-pressure ion source (JEOL instrument). It was discussed above, that the IED in this ion source is not thermal; and that was possible to estimate only empirically, based on the value of KIE. Qualitatively, fragmenting ions have a lower internal energy (indicated by the experimentally determined lower effective temperature values) than in the case of high-pressure ion source. Using this empirical IED, the KER can be determined, applying the aforementioned 'prior distribution' model (Table 1). This should result in a lower KER value. Indeed, the KER value determined experimentally for diethylamine is nearly three times lower using a low pressure than using a high-pressure ion source ($\langle \text{KER} \rangle = 29$ vs. 67 meV, respectively).

In the previous discussions it was shown, that the IEDs for reacting ions in a thermal system and metastable ions characterized by effective temperature are quite similar (Fig. 5). It was also shown, that KER values can be well described by a three-dimensional translational energy distribution ($3/2kT$ in a thermal system). Connecting the two features, the KER and the effective temperature should be connected by the simple equation:

$$\langle \text{KER} \rangle \approx 3/2\, kT_{\text{eff}} \tag{4}$$

Note that the arguments used here are analogous to those of the 'finite heat bath theory' [20,36,37], developed by Klots to describe fragmentation of cluster ions.

Fig. 8 shows the correlation according to the equation above, using T_{eff} (determined from experimentally observed ion ratios using Eq. (2) [9]) and the $\langle \text{KER} \rangle$ values. Figure 8 shows both the experimentally observed and the calculated $\langle \text{KER} \rangle$ values (full circles and open squares, respectively). There is a good linear correlation between T_{eff} and $\langle \text{KER} \rangle$ and the slope is very close to that described by Eq. (4). This correlation is quite significant, as it suggests, that the 'prior distribution' model is a physically reasonable assumption to describe fragmentation of proton-bound alkylamine dimers. It also indicates that (a) KER can be described as a three-dimensional translational motion and suggests that (b) statistical energy partitioning occurs in a late transition state. The linear correlation observed for α-deuterated compounds clearly illustrates that there is a strong connection between the KIE and KER.

A final comparison between experiments and calculations can be made based on the ratio of KER

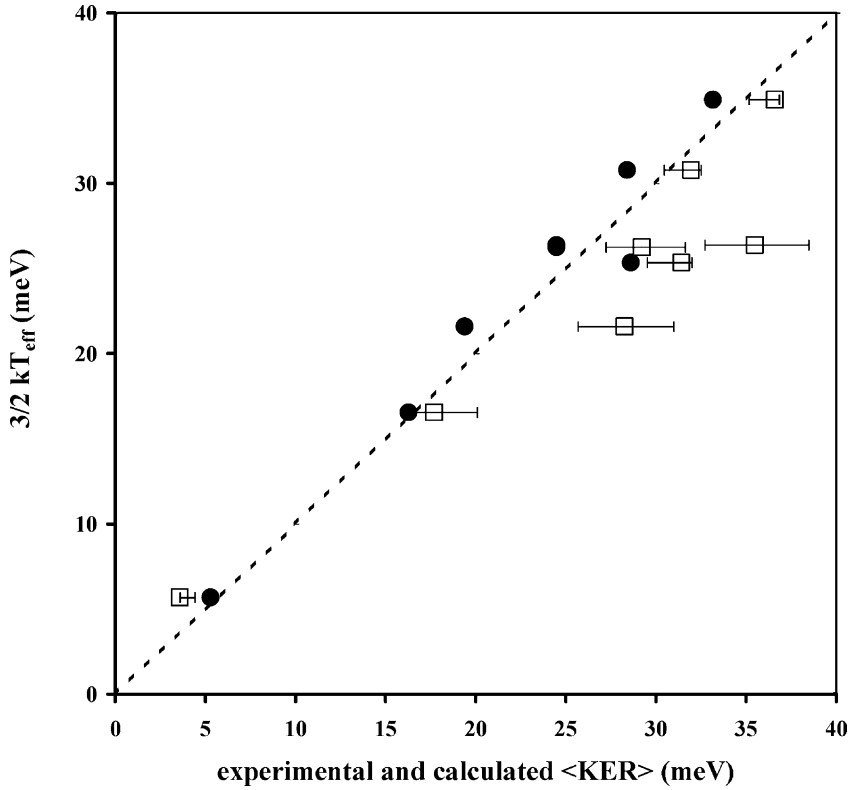

Fig. 8. Correlation between the calculated (open squares) and experimentally measured (full circles) mean kinetic energy release and the effective temperature, calculated using experimentally observed ion ratios, based on Eq. (2). Data are shown for α-D substitution. The expected correlation assuming a three-dimensional translational energy distribution (Eq. (4)) is shown by the broken line (correlation coefficients are 0.979 and 0.952 for experimental and calculated ⟨KER⟩ values, respectively).

observed for the two alternative reaction channels of the dimer, as described by reactions (1a) and (1b). This ratio is given in [9] only for the methylamine system on the JEOL instrument, and it is 1.31. The calculated value is quite similar (1.22), which is a further encouraging sign for the calculations. Calculations suggest that such a large difference can only be expected, when T_{eff} is very low. For the other compounds KER(H) and KER(B) values were nearly equal.

4. Conclusions

In the present paper kinetic isotope effects and kinetic energy release in the dissociation reactions of proton-bound amine dimers are discussed. The experimental results of Norrman and McMahon are compared to model calculations performed by the MassKinetics program. The input parameters are the reaction enthalpy (determined experimentally), vibrational frequencies of the reactant and the products (calculated by high-quality molecular orbital calculations), internal energy distribution in the ion source and a parameter (the pre-exponential factor) characterizing the looseness of the transition state. An empirically determined $\lg A_{preexp} = 15.4$ was used for all compounds. Calculations were repeated using 10 times larger and 10 times lower pre-exponential factors as well, suggesting error limits for the calculations. Note that this 15.4 value is a typical one for loose transition states [18,19,26,47].

In a high-pressure ion source the internal energy distribution should be thermal. In this case not only the direction, but also the degree of the—very small—secondary kinetic isotope effect was successfully modeled, the correlation between experimental and calculated results is shown in Fig. 2. The experimentally determined kinetic energy release was available for one compound only. This was also calculated theoretically, showing a fair agreement with experimental value. It is important to emphasize that the only empirical parameter in these calculations is the pre-exponential factor.

Experiments performed on the JEOL instrument, equipped with a low-pressure ion source, showed significantly larger kinetic isotope effect, and smaller KER values than those obtained on the VG instrument equipped with a high-pressure ion source [9]. This indicates that internal energy distributions obtained using the two ion sources are different. Calculations clearly suggest that this difference cannot be explained by the slightly longer time-scale of the experiments. We suggest that the difference is due to an incomplete thermalization—which seems reasonable in a low-pressure ion source. This explanation accounts both for the higher isotope effect, for the higher abundance of metastable ions and for the smaller KER value. Accepting this, it is easy to model energy distributions empirically: The internal energy distribution was therefore modified using a single parameter to match the measured and the calculated kinetic isotope effect for the JEOL instrument. Using the internal energy distributions so obtained it was possible to calculate the kinetic energy release values for the low-pressure ion source accurately (Fig. 8). The ratio KER(H) and KER(D) values (i.e., those relating to the competing reactions (1a) and (1b)) was determined experimentally for methylamine [9], and it was also calculated as well (1.31 and 1.22 meV, respectively).

A very important finding in the present paper is the simple linear relationship between the kinetic energy release and the effective temperature, expressed as $\langle \mathrm{KER} \rangle = 3/2kT_{\mathrm{eff}}$. Such a correlation can be expected in other systems as well, provided the KER is mainly determined by statistical factors and not by the activation energy of the reverse reaction. This is between data obtained experimentally, but the calculated values show a similar agreement. This also shows that the KER can be described as a three-dimensional translational motion.

Acknowledgements

The authors are indebted to Kion Norrman and Terry McMahon for discussions and for obtaining vibrational frequencies of most studied compounds and to Graham Cooks for his valuable comments.

References

[1] H. Budzikiewicz, C. Djerassi, D.H. Williams, Mass Spectrometry of Organic Compounds, Holden-Day, San Francisco, USA, 1967.
[2] T.T. Dang, E.L. Motell, M.J. Travers, E.P. Clifford, G.B. Ellison, C.H. DePuy, V.M. BierBaum, Int. J. Mass Spectrom. Ion Process. 123 (1993) 171.
[3] P.J. Derrick, Mass. Spectrom. Rev. 2 (1983) 285.
[4] P.J. Derrick, K.F. Donchi, in: C.H. Bamford, C.F.H. Tipper (Eds.), Comprehensive Chemical Kinetics, Elsevier, Amsterdam, 1983.
[5] F.C. Gozzo, M.N. Eberlin, J. Mass Spectrom. 36 (2001) 1140.
[6] M.J. Haas, A.G. Harrison, Int. J. Mass Spectrom. Ion Process. 124 (1993) 115.
[7] S. Ingemann, S. Hammerum, Adv. Mass Spectrom. 8 (1980) 647.
[8] S. Ingemann, S. Hammerum, P.J. Derrick, J. Am. Chem. Soc. 110 (1988) 3869.
[9] K. Norrman, T.B. McMahon, Int. J. Mass Spetrom. 182/183 (1999) 381.
[10] B.D. Nourse, R.G. Cooks, Int. J. Mass Spectrom. Ion Process. 106 (1991) 249.
[11] R.A.J. O'Hair, S. Gronert, T.D. Williams, Org. Mass Spectrom. 29 (1994) 151.
[12] D. Schroder, R. Wesendrup, R.H. Hertwig, T.K. Dargel, H. Grauel, W. Koch, B.R. Bender, H. Schwarz, Organometallics 19 (2000) 2608.
[13] R.G. Cooks, T.L. Kruger, J. Am. Chem. Soc. 99 (1977) 1279.
[14] R.G. Cooks, J.S. Patrick, T. Kotiaho, S.A. McLuckey, Mass Spectrom. Rev. 13 (1994) 287.
[15] R.G. Cooks, J.T. Koskinen, P.D. Thomas, J. Mass Spectrom. 34 (1999) 85.
[16] P.B. Armentrout, J. Mass Spectrom. 34 (1999) 74.
[17] L. Drahos, K. Vékey, J. Mass Spectrom. 34 (1999) 79.
[18] J.L. Holmes, C. Aubry, P.M. Mayer, J. Phys. Chem. A 103 (1999) 705.
[19] P.D. Thomas, R.G. Cooks, K. Vékey, L. Drahos, J. Phys. Chem. A 104 (2000) 1359.

[20] J. Laskin, J. Futrell, J. Phys. Chem. A 104 (38) (2000) 8829.
[21] G. Bojesen, T. Breindahl, J. Chem. Soc. Perkin. Trans. 2 (1994) 1029.
[22] S.L. Craig, M.Z. Zhong, B. Choo, J.I. Braumann, J. Phys. Chem. A 101 (1997) 19.
[23] P.B. Armentrout, J. Am. Soc. Mass Spectrom. 11 (2000) 371.
[24] K.M. Ervin, Int. J. Mass Spectrom. 195/196 (2000) 271.
[25] G. Hvistendahl, E. Uggerud, Org. Mass Spectrom. 26 (1991) 67.
[26] T. Baer, W.L. Hase, Unimolecular Reaction Dynamics, Oxford University Press, New York, 1996.
[27] E. Uggerud, Mass Spectrom. Rev. 18 (1999) 285.
[28] J. Laskin, C. Lifshitz, J. Mass Spectrom. 36 (2001) 459.
[29] D.M. Mintz, T. Baer, J. Chem. Phys. 65 (1976) 2407.
[30] R.G. Cooks, J.H. Beynon, R.M. Caprioli, G.R. Lester, Metastable Ions, Elsevier, Amsterdam, 1973.
[31] Z. Szilágyi, K. Vékey, Eur. Mass Spectrom. 1 (1995) 507.
[32] P. Pechukas, J.C. Light, J. Chem Phys. 42 (1965) 3281.
[33] C.E. Klots, Naturforschung 27 (1972) 553.
[34] W.J. Chesnavich, M.T. Bowers, J. Chem. Phys. 66 (1977) 2306.
[35] W.J. Chesnavich, M.T. Bowers, J. Am. Chem. Soc. 99 (1977) 1705.
[36] C.E. Klots, J. Chem. Phys. 90 (1989) 4470.
[37] C.E. Klots, J. Chem. Phys. 98 (1993) 1110.
[38] J.C. Lorquet, B. Leyh, Org. Mass Spectrom. 28 (1993) 1225.
[39] P. Urbain, F. Remacle, B. Leyh, J.C. Lorquet, J. Phys. Chem. 100 (1996) 8003.
[40] J.C. Lorquet, Int. J. Mass Spectrom. 201 (2000) 59.
[41] P.A.M. van Koppen, M.T. Bowers, C.L. Haynes, P.B. Armentrout, J. Am. Chem. Soc. 120 (1998) 5704.
[42] L. Drahos, K. Vékey, J. Mass Spectrom. 36 (2001) 237.
[43] J. Steinfeld, J. Francisco, W. Hase, Chemical Kinetics and Dynamics, Prentice-Hall, New Jersey, 1989.
[44] P.J. Robinson, K.A. Holbrook, Unimolecular Reactions, John Wiley & Sons Ltd., Bristol, 1972.
[45] I. Oppenheim, K.E. Shuler, G.H. Weiss, Stochastic Processes in Chemical Physic: The Master Equation, MIT Press, Cambridge, 1977.
[46] L. Drahos, R.M.A. Heeren, C. Collette, E.D. Pauw, K. Vékey, J. Mass Spectrom. 34 (1999) 1373.
[47] L. Wua, J.W. Denault, R.G. Cooks, L. Drahos, K. Vékey, J. Am. Soc. Mass Spectrom. 13 (2002) 1386.
[48] R.C. Dunbar, Mass Spectrom. Rev. 11 (1992) 309.
[49] A.D. Becke, Phys. Rev. A38 (1988) 3098.
[50] C. Lee, W. Yang, R.G. Parr, Phys. Rev. B37 (1988) 785.
[51] A.D. Becke, J. Chem. Phys. 97 (1992) 9173.
[52] G. Rauhut, P. Pulay, J. Phys. Chem. 99 (1995) 3093.
[53] A.P. Scott, L. Radom, J. Phys. Chem. 100 (1996) 16502.
[54] M.T. Rodgers, K.M. Ervin, P.B. Armentrout, J. Chem. Phys. 106 (1997) 4499.
[55] L. Drahos, J. Sztáray, K. Vékey, Accurate modeling of mass spectra using MassKinetics, in: Proceedings of the 20th Informal Meeting on Mass Spectrometry, Italy, 2002.
[56] J.L. Holmes, J.K. Terlouw, Org. Mass Spectrom. 15 (1980) 383.